Aesth Plast Surg (2023) 47:2841–2852
https://doi.org/10.1007/s00266-023-03450-8

ORIGINAL ARTICLE BASIC SCIENCE/EXPERIMENTAL

Combined Pulsed Magnetic Field and Radiofrequency Electromagnetic Field Enhances MMP-9, Collagen-4, VEGF Synthesis to Improve Wound Healing Via Hif-1α/eNOS Pathway



Halil Asci[1,2] · Mehtap Savran[1,2] · Selcuk Comlekci[2,3] · Mehmet M. Sofu[2] · Yalcin Erzurumlu[2,4] · Ozlem Ozmen[5] · Mine Kaynak[1] · Mehmet E. Sahin[6] · Rumeysa Taner[2] · Mustafa Gecin[3]

Received: 27 March 2023 / Accepted: 1 June 2023 / Published online: 27 June 2023
© Springer Science+Business Media, LLC, part of Springer Nature and International Society of Aesthetic Plastic Surgery 2023

Abstract

Background The blood supply of the tissue is very important in the acceleration of wound healing. Radiofrequency electromagnetic field (RF) and the pulsed magnetic field (PMF) increase vasodilation to contribute wound healing. The aim of this study was to evaluate the effects of RF and PMF on wound healing via hypoxia-inducible factor-1 alpha (Hif-1α)/endothelial nitric oxide synthase (eNOS) pathway.

Methods Forty-eight rats were divided into 4 groups as sham (wound created only), PMF (27.12 MHz, 12 times a day at 30-min intervals), RF (0.5 mT, continuously) and PMF + RF groups. Wounds were created at 1.5 × 1.5 cm size to the dorsal region, and animals were put into unit. Six animals were killed on days 4 and 7; wound tissues were collected for histopathological, immunohistochemical as collagen-4, cytokeratin, matrix metalloproteinase-9 (MMP-9), vascular endothelial growth factor (VEGF) staining and Hif-1α/eNOS/VEGF expressions.

Results On day 4, in addition to increasing VEGF and MMP-9 stainings, connection between intact tissue and scar tissue which was stronger in the RF- and PMF-applied groups was observed. On day 7, epithelization started; inflammatory reaction decreased; collagen production, cytokeratin, VEGF and MMP-9 expression enhanced, especially in the RF + PMF applied group. eNOS, Hif-1α and VEGF expression levels were found to be significantly highest in both days of RF + PMF-applied group.

Conclusions This study revealed that both in vitro RF and PMF applications can cause notable changes in factors that are required for tissue repair on wound healing such as epithelization, connective tissue formation, collagen

✉ Halil Asci
halilasci@sdu.edu.tr

Mehtap Savran
mehtapsavran@sdu.edu.tr

Selcuk Comlekci
scom56@gmail.com

Mehmet M. Sofu
mehmetsofu@sdu.edu.tr

Yalcin Erzurumlu
yalcin.erzurumlu@gmail.com

Ozlem Ozmen
ozlemoz@mehmetakif.edu.tr

Mine Kaynak
mine.kaynak37@gmail.com

Mehmet E. Sahin
erhansahin@isparta.edu.tr

Rumeysa Taner
rumeysataner21@gmail.com

Mustafa Gecin
mustafagecin@sdu.edu.tr

[1] Department of Pharmacology, Faculty of Medicine, Suleyman Demirel University, Isparta, Turkey

[2] Department of Bioengineering, Institute of Science, Suleyman Demirel University, Isparta, Turkey

[3] Department of Electronics and Communication Engineering, Faculty of Engineering, Suleyman Demirel University, Isparta, Turkey

[4] Department of Biochemistry, Faculty of Pharmacy, Suleyman Demirel University, Isparta, Turkey

[5] Department of Pathology, Faculty of Veterinary Medicine, Burdur Mehmet Akif Ersoy University, Burdur, Turkey

[6] Department of Biomedical Device Technology, Technical Sciences Vocational High School, Isparta University of Applied Sciences, Isparta, Turkey

production and angiogenesis via vasodilatory Hif-1α/eNOS pathway and VEGF signaling.
No Level Assigned This journal requires that authors assign a level of evidence to each submission to which Evidence-Based Medicine rankings are applicable. This excludes Review Articles, Book Reviews, and manuscripts that concern Basic Science, Animal Studies, Cadaver Studies, and Experimental Studies. For a full description of these Evidence-Based Medicine ratings, please refer to the Table of Contents or the online Instructions to Authors www.springer.com/00266.

Keywords Wound healing · Radiofrequency electromagnetic field · Pulsed magnetic field · Hif-1α · eNOS

Introduction

The skin is a specialized structure for interfacing with the external environment and provides many important homeostatic functions, from regulating thermostability to sensing external stimuli. It acts as a mechanical barrier, and when its integrity becomes disrupted, rapid repairing processes initiate known as wound healing [1].

The wound healing process includes three consecutive and overlapping steps: hemostatic/inflammatory, proliferative and remodeling stages. Fully integrated wound healing involves the cooperative interactions of multiple cell types, various growth factors, cytokines and chemokines [2–4]. These interactions result in neutrophilic infiltration, elimination of foreign substances in the acute state and wound contraction to maintain tissue stability [5–8]. Disruption of this process could delay or obstruct wound healing.

To accelerate these effects, various substances and methods with different mechanisms are tried [9]. Inadequate efficacy observed in chemical wound healing studies and the emergence of drug-related side effects create limitations in the field of use [10]. The systems used in in-vitro methods are generally tried to increase the migration of cells involved in the healing process to the wound surface with the effects of chemoattractants [11].

Electrical methods that accelerate wound healing are inadequate to provide complete restoration. Currently, there are not enough studies on the combined application of these methods. Therefore, using combined therapeutic electrical methods is an innovative idea.

Radiofrequency electromagnetic field (RF) contributes to vasodilation by increasing endothelial nitric oxide synthase (eNOS) mediated nitric oxide (NO) synthesis from the endothelial layer of vascular structures in the area where it is applied. Bragin et al. found that 27.12 MHz frequency enhances the production of eNOS-related NO synthesis in rat brain [12]. eNOS synthesis mediated by hypoxia-inducible factor-1 alpha (Hif-1α) is a pathway that has been investigated in many disease models that require vasodilation such as wound healing [13]. Also, it increases the synthesis of tissue growth factors such as vascular endothelial growth factor (VEGF) by using the same intracellular pathway [11].

The pulsed magnetic field (PMF) can increase the synthesis of the molecules used in wound healing, especially collagen synthesis, as well as the migration of the cells to the damaged area depending on the electrostatic charges [14]. The intracellular action mechanism of this method's effect on the hypoxia-inducible factor-1 alpha (Hif-1α) pathway has not been investigated yet.

Researching and developing novel treatment methods have always been on the agenda of scientific literature. According to that motive, comparing the above-mentioned effects of single and combined applications of RF and PMF on wound healing and the Hif-1α/eNOS pathway is the main purpose of this study.

Materials and Methods

Ethical Approval and Animals

Wistar albino type adult female rats (n = 48, 8–10 weeks old, 250–350 g) obtained from Suleyman Demirel University Experimental Animal Production and Experimental Research Laboratory were used. The study was approved by the Suleyman Demirel University Experimental Animals Local Ethics Committee (Ethics No: 27.12.2019/14-02). This study was supported by KOSGEB (project code 55FG1) and Suleyman Demirel University Scientific Research Projects Coordination Unit (project code TSG-2022-8783). The animals were housed in a standard laboratory environment with constant temperature and humidity for 12:12 h, light–dark cycle, and 55–60% humidity for 8–10 days. During the shelter, the experimental animals were subjected to standard feeding, housing and care conditions.

Study Design and Preparation of Wound Area

Forty-eight rats were divided into 4 groups 12 rats of each as sham (wound created only), PMF, RF and PMF+RF groups. On day 1, under 80–100 mg/kg ketamine (Ketalar, Pfizer, Turkey) and 10 mg/kg xylazine (Xylazinbio %2, Bioveta, Czech Republic) anesthesia, back area of the rats shaved widely. After proper disinfection with a batticon, 1.5 × 1.5 cm size wounds were created with a scalpel of the specified sizes by removing cutaneous and

subcutaneous tissues. Then, wounds were closed with sterile dressing materials. After that, rats were put into cages and taken to RF and PMF exposed area.

Six animals were killed from each group, under the same doses of anesthesia on days 4 and 7. After the killing, the half of the wound tissues put into 10% formaldehyde for histopathological and immunohistochemical examination as collagen-4, cytokeratin, matrix metalloproteinase-9 (MMP-9), VEGF staining. Remaining tissues put into the aluminum foil with regard to cold chain for PCR analyses of VEGF/Hif-1α/eNOS expressions. Details of experimental protocol are given in Fig. 1.

RF Setup and PMF Applications

RF device conducted with 27.12 MHz operated for 12 shifts a day of 30 min on/1.5 h off periods and PMF device conducted with 0.5 mT applied continuously during the experimental procedure [12, 14].

It is observed that the magnetic field was quite homogeneous in the environment suitable for the dimensions of the Euro type-2 cage and 30 mm above the bottom of the cage by using electromagnetic stimulations (CST Studio Suite 3D simulation, Oxford shire, UK). The 27.12-MHz RF applicator with a targeted electric field value of 10 V/m. To achieve this exposure, we had to feed the circuit by 12 V_{dc}. In this circumstance, we got 0.8 W of RF output from the PCB antenna.

The second part of the exposure system was aimed magnetic field strength value of 0.5 mT occurred "exposure environment" for rats by using a two-coil set under each cage (Fig. 2).

All RF and PMF field measurements have been carried out by using a field meter (Mustool MT-525, China), (ELF meter PF-4, UK), (Extech 480836, USA).

The experiments were started by feeding and adjusting the circuits to give the target 10 V/m electric field density on each cage. Spectrum analysers (ROHDE-SCHWARZ FSH6, USA, PROMAX AE-566 spectrum analyser, USA) were used at every stage of the experimental steps. In the scientific literature, it is emphasized that such exposure mechanisms should be isolated from the external environment. For this reason, the shielding efficiency of the electromagnetically isolated room (clean room) of the Suleyman Demirel University Animal Experiments Laboratory where the experiments were carried out was measured as (80 dB) for this operating frequency (27.12 MHz).

Histopathological Analyses

At the end of the investigation, the wound region samples were collected and fixed in 10% neutral formalin during the necropsy for histological and immunohistochemical examinations. After 2 days of fixation, skin samples were routinely processed by a fully automated tissue processor (ASP300S; Leica, Wetzlar, Germany). Following the paraffin wax embedding of the tissues, 6 serial sections of 5 μm thickness were cut from the paraffin blocks using a rotary microtome (RM2155; Leica). Hematoxylin and eosin (HE) was used to stain a series of sections for histopathological analysis, and the slides were coverslipped and examined using a light microscope.

The other serial sections were stained using Picro Sirius Red method for collagen (ab150681, Abcam, UK) to evaluate connective tissue healing according to manufacturer instructions and examined under a light microscope. Microphotography and morphometric analyses were performed using the Database Manual Cell Sens Life Science Imaging Software System (Olympus Corporation, Tokyo, Japan).

Immunohistochemical Analyses

Selected sections were immunostained with collagen-4 (Collagen 4 polyclonal antibody (bs-4595R) Bioss Antibodies Inc., Massachusetts USA); cytokeratin (Cytokeratin 1 (4D12B3): sc-65999) Santa Cruz); matrix metalloproteinase (MMP)-9 (MMP-9 (7-11C) (sc-13520) Santa Cruz); and VEGF (VEGF (C-1) (sc-7269) Santa Cruz, Texas, USA) by streptavidin–biotin technique. All primary antibodies were used as 1/100 dilution. The sections were incubated with the primary antibodies for 60 min, and immunohistochemistry was carried out using a biotinylated secondary antibody and streptavidin–alkaline phosphatase conjugate. UltraVision Detection System Anti-Polyvalenti HRP kit (TP-060-HL) (Thermo Shandon Limited, Cheshire, UK) was used as a secondary antibody. The antigens were demonstrated by using diaminobenzidine (DAB) as the chromogen. For negative controls, the primary antiserum step was omitted. All examinations were performed on blinded samples.

All the slides were analyzed for immunopositivity, and semi-quantitative analyses were carried out. Samples were analyzed by examining five different sections in each sample, which were then scored from 0 to 3 according to the intensity of staining (0, absence of staining; 1, slight; 2, medium; 3, marked staining). The morphometric evaluation was made by using the database.

Genetic Analyses

Analyses of Relative mRNA expression by Quantitative Real-Time Polymerase Chain (qRT-PCR) Total RNA Extraction and Purification

Total RNA was extracted from rat tissues by using TRIzol™ Reagent (Thermo Fisher Scientific, California)

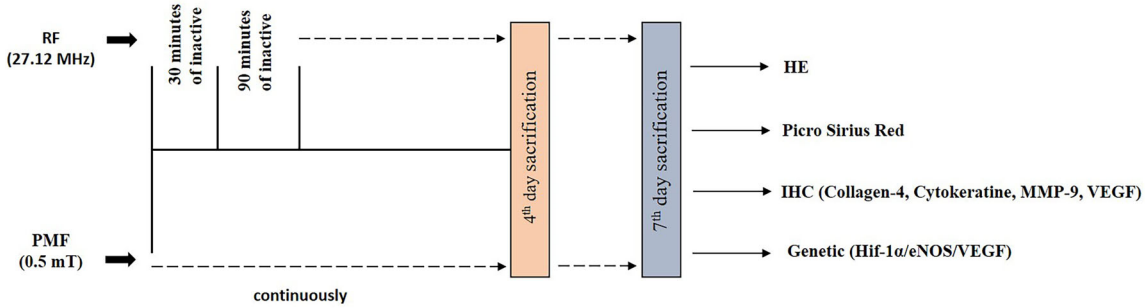


Fig. 1 Summary of the experimental protocols for this study. RF: radiofrequency electromagnetic field; PMF: pulsed magnetic field; eNOS: endothelial nitric oxide synthase; VEGF: vascular endothelial growth factor; MMP-9: matrix metalloproteinase; Hif-1α: hypoxia-inducible factor-1 alpha; HE: hematoxylin–eosin; IHC: immunohistochemistry

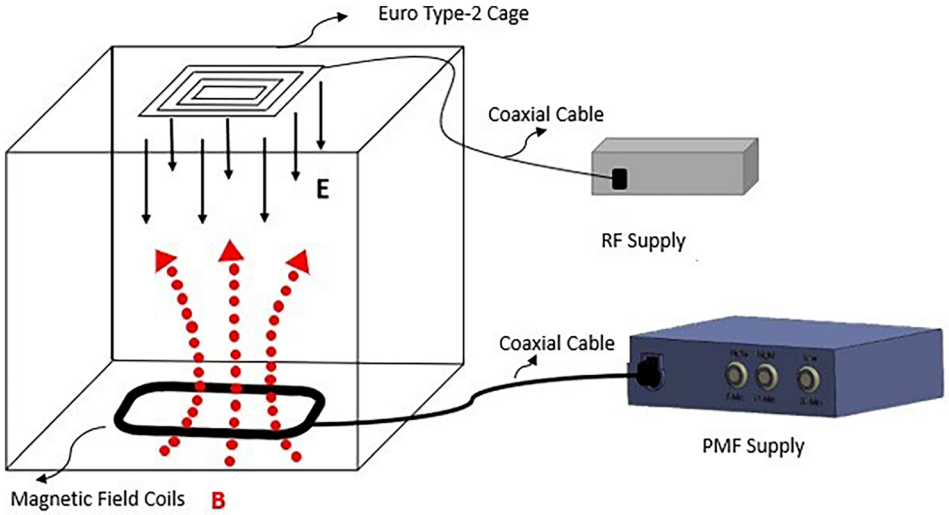


Fig. 2 Schematic view of the experimental setup. E: radiofrequency electromagnetic field, B: pulsed magnetic field

following the manufacturer's instructions. RNA concentration and purity were determined by the MySPEC microvolume spectrophotometer (VWR).

cDNA Synthesis

Total RNA (1 μg) was reverse transcribed with the iScript cDNA Synthesis kit by using oligo dT primers (Bio-Rad Laboratories, Hercules, California). The reaction mix was incubated for 5 min at 25 °C, for 20 min at 46 °C and 1 min at 95 °C.

qRT-PCR

qRT-PCR amplification was performed using iTaq Universal SYBR Green Supermix (Bio-Rad Laboratories, Hercules, California) in the CFX96 instrument (Bio-Rad Laboratories, Hercules, California) according to the manufacturer's instructions.

Specific primers were designed against VEGF, Hif-1α, eNOS and glyceraldehyde-3-phosphate dehydrogenase (GAPDH). eNOS (forward 5'GTGAAGGCGACTATCCTGTATG 3′, reverse 5′ CATGCTCTAGGGATACCACATC3'), Hif1α (forward 5'GGAAATG CTG GCTCCCTATATC3', reverse 5'GTAACTGGGTCTG CTGGAATC3'), VEGF (forward 5'GGAAGAGAGA GAGAGAGAGAGAC3', reverse 5'GACTGGTCC GATGAAAGATCC 3') GAPDH (forward 5'CAAGGTCATCCCAGAGCTGAA3', reverse 5'CATGTAGGCC ATGAGGTCCAC3'). cDNA samples were analyzed in triplicates for each PCR. The expression of GAPDH was used to normalize cDNA levels. The following PCR conditions were used: denaturation at 95 °C for 10 min, followed by 45 cycles of 10 s at 95 °C and 30 s at 60 °C. Relative quantification of gene expression was performed using the comparative $^{\Delta\Delta}$Ct method. The PCR products were analyzed by a melting curve to ascertain the specificity of amplification.

Statistical Evaluation

Variables were presented as mean ± standard deviation. One-way ANOVA and post hoc LSD tests were used to compare the genetic, histopathological and

immunohistochemical scores between the groups. The calculations were made using the SPSS 18.0 (SPSS Inc., Chicago, IL, USA) program package. $p<0.05$ was set as the significance value.

Results

Histopathological Results

On day 4, it was discovered that the wound region had begun to build a crust and that a pronounced inflammatory cell reaction—dominated mostly by neutrophils with edematous connective tissue—had grown. During the examination of tissue sections, it was observed that the connection between the normal and the lesioned region was slightly occurred in all of the rats in the sham group, and the connection was stronger in the RF and PMF+RF groups. Yet, there was no significant difference in the groups' reactions (Fig.3).

At the histopathological examination of the wound area on day 7, significant inflammatory changes were also observed in the sham group. The newly formed connective tissue could not be securely attached to the normal tissue since epithelization was not formed and there was a significant inflammatory reaction on the wound surface. In the other groups, connective tissue was formed clearly and a tight connection with normal tissue was formed. Especially in the PMF+RF group, epithelization started successfully, inflammatory reaction decreased, connective tissue began to change the mature fibrous tissue and significant wound healing occurred. It was noticed that the skin defects of many rats in the PMF+RF group were mostly closed and ameliorated (Fig. 4).

At the examination of sections stained with Picro Sirius Red method, it was noted that there was no significant collagen production in the sham group on days 4 and 7. In the other groups, collagen production drew attention which started on the 4th day of wound healing and became more distinct on day 7. It was observed that collagen production increased significantly in the peripheral parts of the lesions in the PMF+RF group (Figs. 3, 4).

Immunohistochemical Results

When the *collagen 4* expression was examined on days 4 and 7, it was observed that the expression was significantly lower in the sham group compared to the other groups for both days. In the RF, PMF and PMF+RF groups, when the same periods were compared among themselves, it was noted that the most significant production was formed in both cells and intercellular regions in the PMF+RF group (Fig. 5).

At the evaluation of *cytokeratin* immune reaction, complete keratinization was not observed in any group on day 4, but epithelial proliferation under the crusts was observed. Cytokeratin expression by the newly formed epithelial cells was slighter in the sham group compared to the other groups (Fig. 5). On day 7, epithelization was formed on the wound area in all groups, but it was more prominent in the PMF and PMF + RF groups (Fig.5). Cytokeratin immuno-expression was significantly higher in all device groups compared to the sham group on both days; also keratinization was observed in the PMF+RF group on day 7 (Fig. 5).

When the *MMP-9* immune reactions were examined, expressions were observed from the 4th day in the PMF and PMF+RF groups and the 7th day in the RF group (Fig. 6).

At the evaluation of the *VEGF* immune reaction, it was observed that expressions seen on day 4 increased significantly in all groups on day 7. It was noteworthy that the highest increment was in the PMF+RF group (Fig. 6).

Positive changes in the wound healing process were observed in all device groups compared to sham in all parameters in the immunohistochemistry evaluations. The most significant changes were observed in the PMF+RF group. Immunohistochemical scores are shown in Table 1.

PCR Results of eNOS, Hif-1α, and VEGF mRNA Expressions

On day 4, the expression level of eNOS was found to be significantly highest in the PMF+RF group ($p \leq 0.001$, $p \leq 0.001$, and p: 0.041, respectively). Also, eNOS levels increased significantly in PMF and RF groups compared to the sham group (p: 0.032 and p: 0.028, respectively).

Hif-1α expression levels were also significantly highest in the PMF+RF group ($p \leq 0.001$, p: 0.035, and p: 0.043, respectively). Similar to eNOS results, Hif-1α levels also increased significantly in PMF and RF groups compared to the sham group (p: 0.027 and p: 0.029, respectively).

VEGF expression levels were found to be significantly increased in all device groups compared to sham (p: 0.046, $p \leq 0.001$, $p \leq 0.001$, respectively). Expression levels in PMF+RF groups were significantly higher compared to the PMF group (p: ≤ 0.001) (Fig. 7).

On day 7, eNOS, Hif-1α and VEGF expression levels significantly increased in all groups compared to the sham group ($p< 0.05$ for all). For all three markers, the expression levels were found to be significantly highest in the PEMF+RF group ($p < 0.05$ for all) (Fig. 7).

All genetical results across the study groups are shown in Table 2.

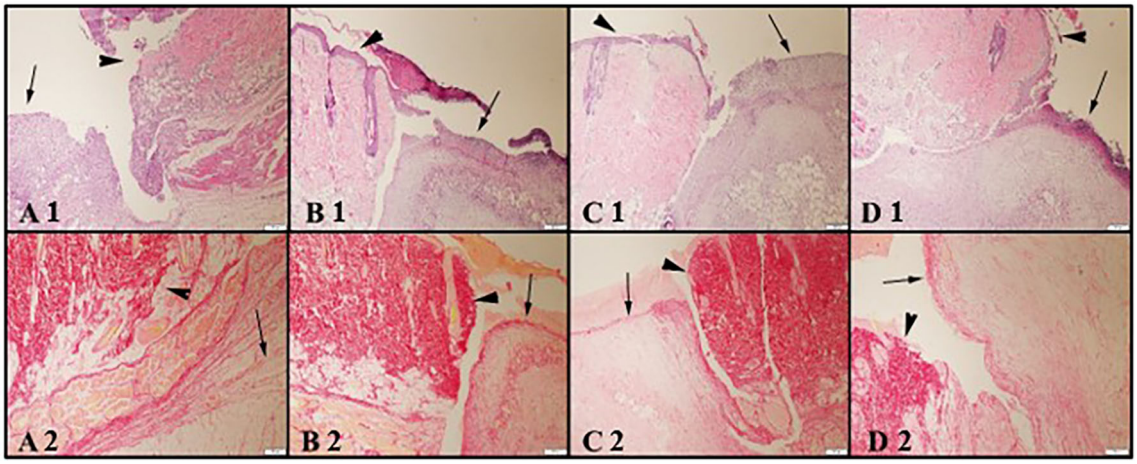


Fig. 3 Histopathological appearance of wound healing on day 4 according to the groups. Inflammatory cell infiltrations (arrows) edematous connective tissue and epidermal healing (arrow heads) in the wound area in **A** Sham group; **B** RF group; **C** PMF group; **D** PMF+RF group. (1) Microscopical appearance of wound healing on day 4 according to the groups (HE); (2) histopathological view of the connective tissue development between the groups on day 4, HE. Normal fibrous tissue around the lesions (arrowheads) and newly proliferated connective tissue (arrows) (Picro Sirius), bars = 200 μm.

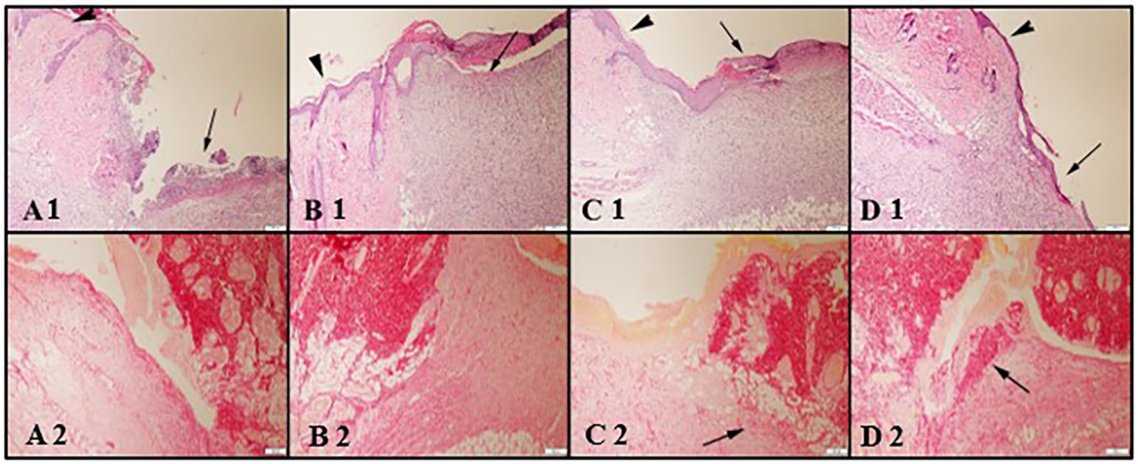


Fig. 4 Histopathological appearance of wound healing on day 7 according to the groups. Inflammatory cell infiltrations(arrow), edematous connective tissue and epithelization (arrows) in the wound area in **A** Sham group; **B** RF group; **C** PMF group; **D** PMF+RF group. (1) Histopathological appearance of wound healing on day 7 according to the groups on day 7 (HE); (2) microscopical view of the connective tissue development and maturation with collagen (arrow) between the groups on day 7 (Picro Sirius), bars = 200 μm.

Discussion

The wound healing mechanism is a common process in almost every pathology. Therefore, treatment methods used for this process are very important [15, 16]. To date, many antioxidant and proliferative and remodeling agents, antibacterial molecules including silver, and active components with vasodilator effects were used to improve wound healing. By these molecules, some processes as to reach an increment in cell proliferation and blood flow, migration of the required cells to the wound area and extracellular matrix synthesis were aimed. Intended changes were mainly occur through increased eNOS [17]. A brief summary about the clinical applications used for wound healing is shown with a schematic illustration in Fig. 8. However, despite all approaches, the majority of which are pharmacological applications, sufficient efficacy and acceleration cannot be achieved in the recovery period and the hospitalization time increases. This situation causes more complicated pathologies due to hospital-acquired infections and thus increases mortality [18].

Critical steps of the wound healing process include the migration of repair cells, collagen synthesis, epithelialization and connective tissue formation [19, 21]. Based on this information, we evaluated these processes with different analyzing methods. Evaluating all the above-mentioned steps constitutes the main strength of this study. In

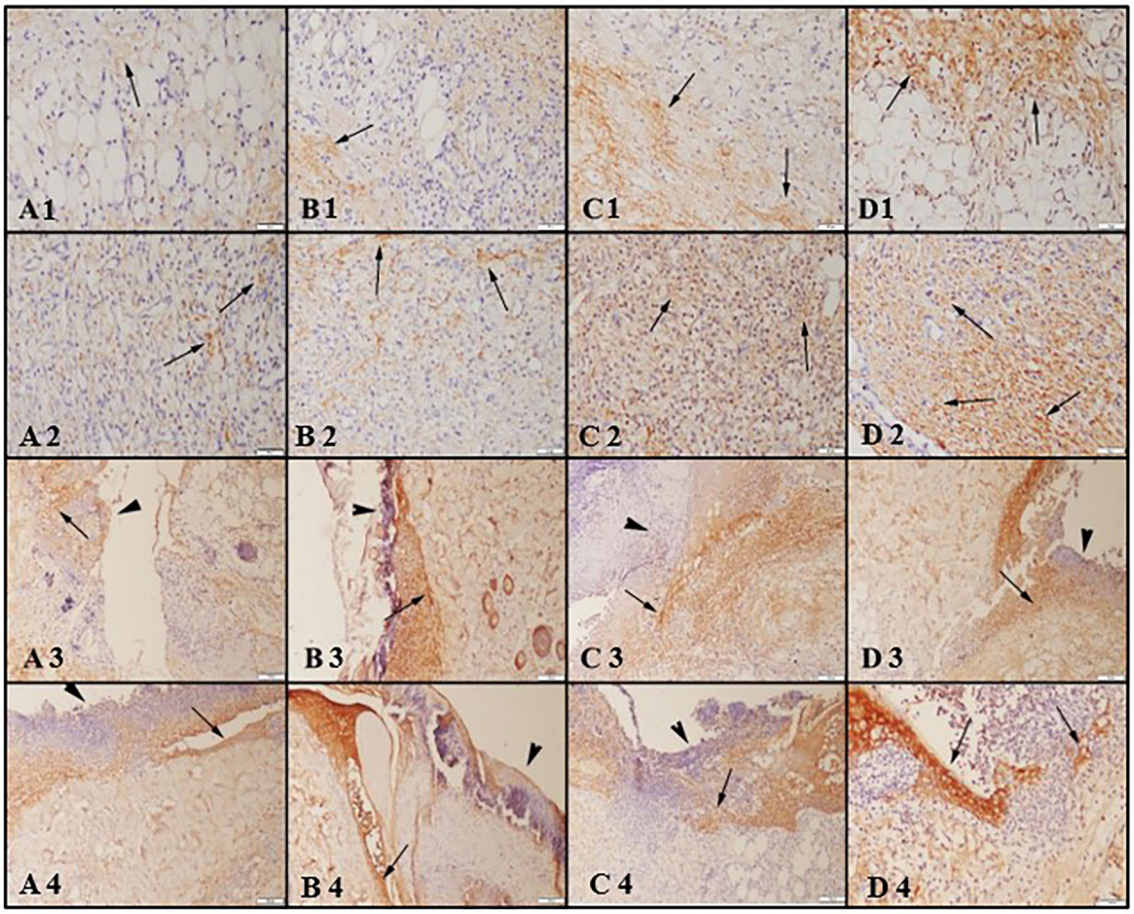


Fig. 5 Collagen-4 and cytokeratin expressions between the groups on days 4 and 7. Expressions showing a significant increase from day 4 **A** Sham; **B** RF; **C** PMF; **D** PMF + RF groups, (1) Collagen-4, day 4; (2) collagen-4, day 7; (3) cytokeratin, day 4; (4) cytokeratin, day 7. Arrows indicate immunopositive cells, and arrow heads indicate crusts and bacterial clusters, Streptavidin–biotin method, bars = 200 μm.

addition, the evaluation of the two methods used in separate groups will contribute to the literature in terms of comparison with their use in combination. On the contrary, a few limitations can be listed: (1) The potential differences of the combined method on male rats need to be evaluated. (2) Markers evaluated by immunostaining should also be assessed by qualitative methods like genetical analyses. (3) Results need to be supported by different analyzing methods.

Although there are studies investigating the effect of RF application on different cellular mechanisms, the same cannot be said for the PMF application. In the experimental model created within the scope of this study, it was important to examine the effects of both methods on days 4 and 7 in terms of comparing the acute–chronic effects. Through that, this study demonstrates our aim to evaluate the time-dependent effectiveness of our innovative method of wound healing.

Neutrophilic inflammatory reactions, an important component of acute phase in wound healing, observed on the 4th day were evident in all groups, but the connections between intact and scar tissues were more evident in the device groups, giving the impression that tissue integrity developed more rapidly with combined PMF + RF applications in the early period. It shows that with the middle area of the wound where cellular proliferation occurs, penetration of intact tissue and thus healing can be accelerated. In addition, the increase in inflammatory cell migration to the wound area, as a result of vasodilatory effect, also explains the increase in the repair rate. This effect may be beneficial for the clearance of foreign bodies in the injured areas. It is clear that the desired epithelialization, tissue integrity and newly developed connective tissue formation can contribute to the mentioned wound healing processes, especially in the combined method groups on the 7th day.

Collagen is an important skin component, needed especially in the proliferation phase of wound healing that is seen in days and weeks following the injury and that stimulates immune cells and fibroblasts to reach the wound

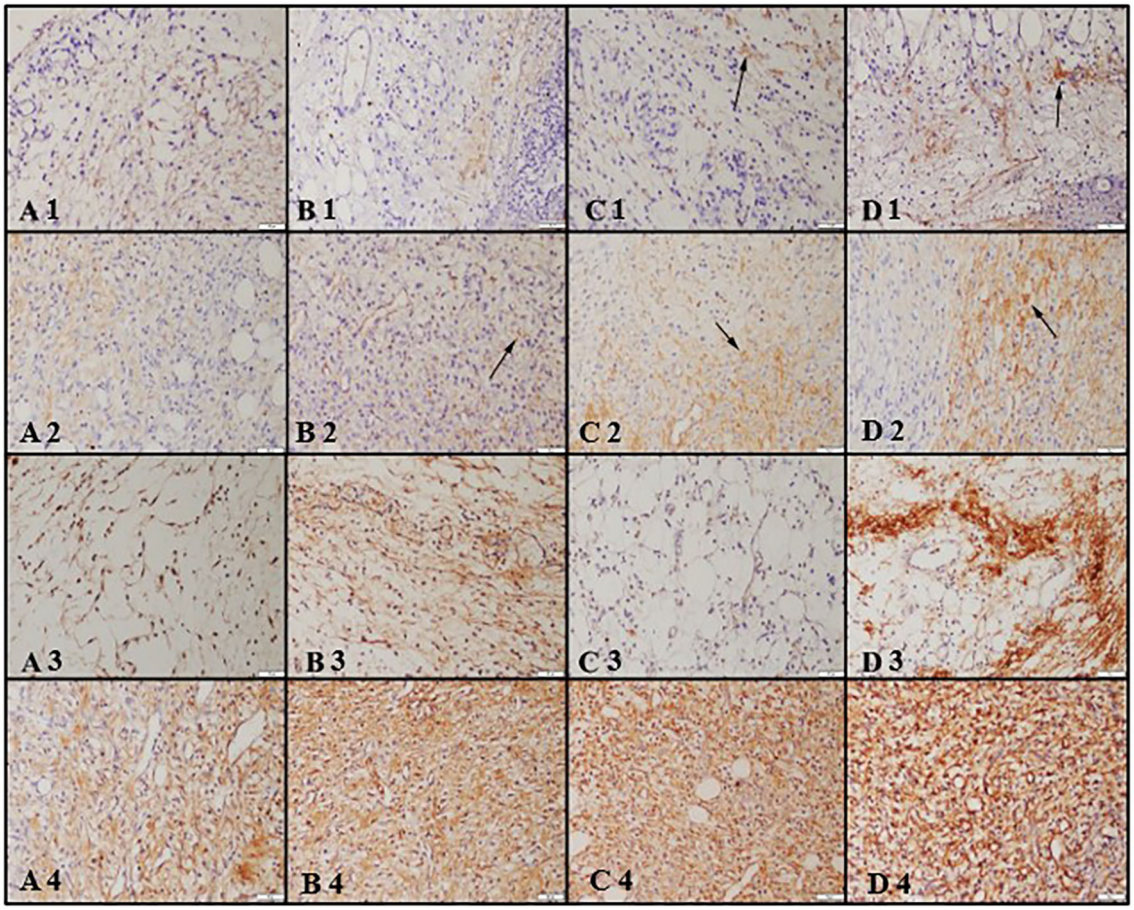


Fig. 6 MMP-9 and VEGF expressions between the groups on days 4 and 7. Expressions showing a significant increase from day 4 **A** Sham; **B** RF; **C** PMF; **D** PMF+RF groups, (1) MMP-9, day 4; (2) MMP-9, day 7; (3) VEGF, day 4; (4) VEGF, day 7. Arrows indicate immunopositive cells. Streptavidin–biotin method, bars = 200 µm.

Table 1 Statistical analysis results of the immunohistochemical scores.

Groups		Collagen	Cytokeratın	MMP-9	VEGF
SHAM	Day 4	0.20 ± 0.20^{a}	0.40 ± 0.24^{a}	0.20 ± 0.20^{a}	0.80 ± 0.44^{a}
	Day 7	0.40 ± 0.24^{a}	$1.00 \pm 0.70^{a,b}$	0.40 ± 0.24^{a}	$1.40 \pm 0.54^{a,b}$
PMF	Day 4	$1.40 \pm 0.54^{b,c}$	$1.20 \pm 0.44^{a,b}$	0.60 ± 0.24^{a}	1.00 ± 0.70^{a}
	Day 7	1.80 ± 0.83^{c}	$2.40 \pm 0.54^{c,d}$	$1.00 \pm 0.70^{a,b,c}$	$2.20 \pm 83^{b,c}$
RF	Day 4	$0.80 \pm 0.37^{a,b}$	1.40 ± 0.54^{b}	0.60 ± 0.24^{a}	$1.60 \pm 0.54^{a,b}$
	Day 7	$1.40 \pm 0.54^{b,c}$	$1.80 \pm 0.83^{b,c,d}$	$0.80 \pm 0.37^{a,b}$	2.40 ± 0.54^{c}
PMF+RF	Day 4	$1.40 \pm 0.54^{b,c}$	$1.60 \pm 0.54^{b,c}$	$1.60 \pm 0.54^{b,c}$	2.60 ± 0.54^{c}
	Day 7	1.80 ± 0.83^{c}	2.60 ± 0.54^{d}	1.80 ± 0.44^{c}	2.80 ± 0.44^{c}
P value		< 0.001	< 0.001	< 0.001	< 0.001

Values are presented as mean ± SD. The relationships between groups and results of histopathological and immunohistochemical scores are assessed by one-way ANOVA.

PMF: pulsed magnetic field; RF: radiofrequency electromagnetic field; VEGF: vascular endothelial growth factor; MMP-9: matrix metalloproteinase-9. The differences between the means of groups carrying different letters in the same column is statistically significant

area, thus protecting the natural extracellular matrix structure and promoting healing. [22, 23]. So, collagen can be added to wound dressing materials to provide structural support or in addition to substances used in many wound healing studies [24, 26]. In this study, endogenous collagen production was not sufficient on the wound surfaces on the

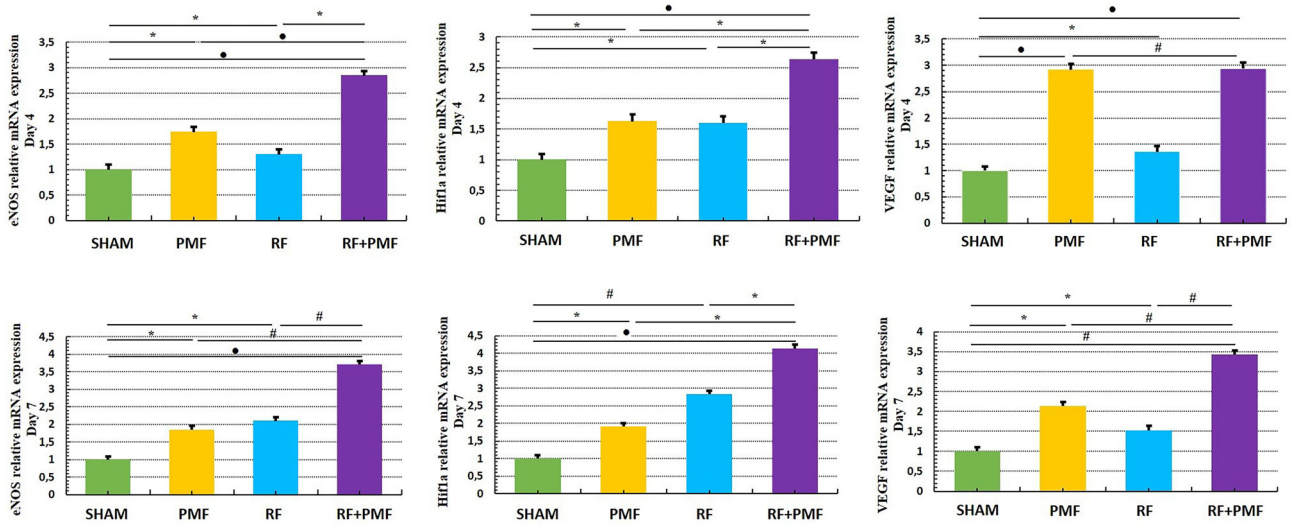


Fig. 7 Quantitative real-time PCR analysis for eNOS, Hif-1α, and VEGF mRNA expressions on days 4-7 between the groups. PMF: pulsed magnetic field; RF: radiofrequency electromagnetic field; eNOS: endothelial nitric oxide synthase; VEGF: vascular endothelial growth factor; Hif-1α: hypoxia-inducible factor-1 alpha. *:p<0,05; #:p<0,01; ●:p<0,001.

Table 2 Genetical results across the study groups

		SHAM	PMF		RF		PMF+RF	
		Mean ± SD	Mean ± SD	*P* value	Mean ± SD	*P* value	Mean ± SD	*P* value
eNOS	Day 4	1.00 ± 0.10	1.30 ± 0.10[a]	a:0.032	1.73 ± 0.09[a]	a: 0.028	2.84±0.08[a,b,c]	a: < 0.001
								b: < 0.001
								c: 0.041
Hif-1α		1.00 ± 0.09	1.62 ± 0.11[a]	a: 0.027	1.59±0.11[a]	a: 0.029	2.63±0.10[a,b,c]	a: < 0.001
								b: < 0.035
								c: 0.043
VEGF		1.00 ± 0.08	1.35 ± 0.10[a]	a: 0.046	2.91±0.11[a]	a: 0<0.001	2.93±0.10[a,b,c]	a: < 0.001
								b: < 0.001
								c: 0.061
eNOS	Day 7	1.00 ± 0.09	2.09 ± 0.10[a]	a: 0.038	1.84 ± 0.18[a]	a: 0.042	3.70±0.10[a,b,c]	a: < 0.001
								b: < 0.001
								c: < 0.001
Hif-1α		1.00 ± 0.10	2.83 ± 0.09[a]	a: <0.001	1.90 ± 0.10[a]	a: 0.035	4.12 ± 0.11[a,b,c]	a: < 0.001
								b: 0.042
								c: 0.036
VEGF		1.00 ± 0.09	1.51 ± 0.11[a]	a: 0.041	2.13 ± 0.10[a]	a: 0.031	3.43 ± 0.09[a,b,c]	a: < 0.001
								b: < 0.001
								c: <0.001

Values are presented as mean ± SD. The relationships between groups and results of histopathological and immunohistochemical scores are assessed by one-way ANOVA. PMF: pulsed magnetic field; RF: radiofrequency electromagnetic field; eNOS: endothelial nitric oxide synthase, Hif-1α: hypoxia-inducible factor 1 alpha, VEGF: vascular endothelial growth factor. "a" comparison with SHAM, "b" comparison with PMF, "c" comparison with RF

4th and 7th days in no-device group. However, with RF and PMF applications, collagen synthesis was found to be more pronounced on the 4th and 7th days compared to the sham group. This is seen as an important development in terms of assessing tissue integrity and the robustness of scar tissue. The fact that this synthesis is observed

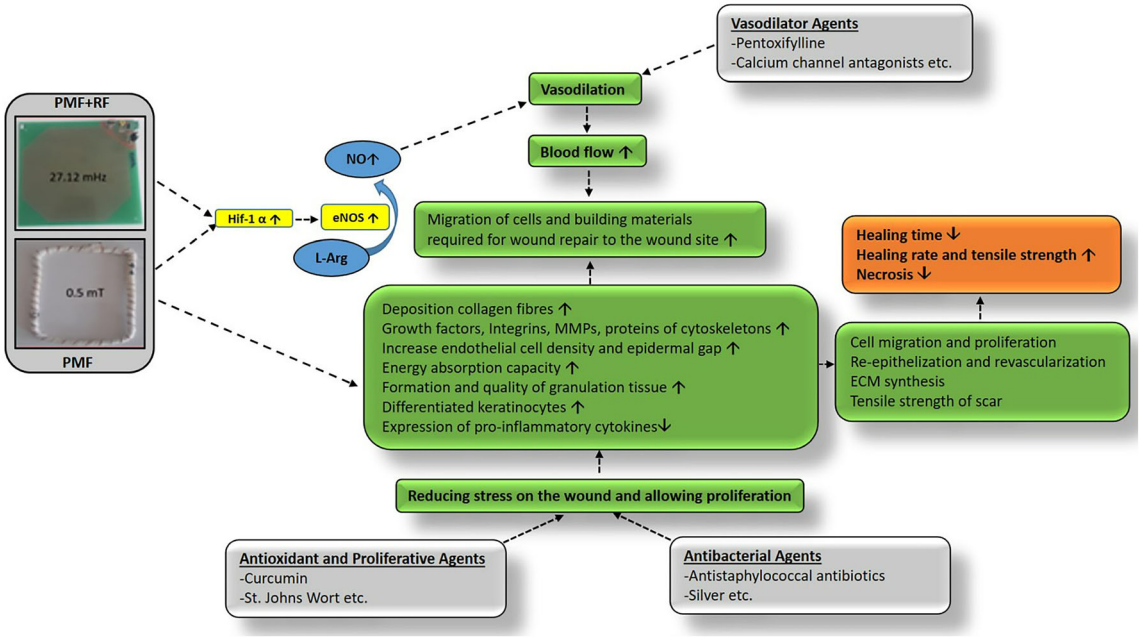


Fig. 8 A brief summary about the clinical applications used for wound healing. RF: radiofrequency electromagnetic field; PMF: pulsed magnetic field; eNOS: endothelial nitric oxide synthase; Hif-1α: hypoxia-inducible factor-1 alpha; NO: nitric oxide; L-Arg: L-arginine

especially in the peripheral part of the wound, which is close to the intact tissue, explains that the connection points are stronger. To evaluate the wound contraction more accurately, long-term studies are needed. In addition, in parallel with the results of the Picro Sirius Red method in immunohistochemical staining, the highest collagen-4 expression observed in both days of combined use supports that the device increases collagen synthesis.

Keratinization is an important part of the proliferation phase in wound healing seen in chronic period, and cytokeratin levels are an important indicator of keratinization in scar tissue. In context of this, it was considered normal that no cytokeratin staining was observed in any groups on day 4. On day 7, especially PMF application increased the cytokeratin expression in PMF and PMF+RF groups compared to others, giving the impression that the effect of PMF on keratinization could be more outstanding.

MMPs are classified according to their substrate specificity and include collagenases (MMPs 1, 8, 13), gelatinases (MMPs 2, 9), matrilysins (MMPs 7, 11, 26), and stromelysins (MMPs 3, 10). Certain MMPs, such as MMP-2 and MMP-9, are localized at the epithelial-stromal interface behind migrating epithelial cells in wounds [27]. Under normal physiological conditions, MMPs are produced in connective tissue for embryonic growth, tissue morphogenesis and growth continuity, and studies showing their role in tissue restructuring have been reported. MMP-9 is typically activated during pathological conditions and produced by different cell types, including macrophages and neutrophils, and plays a variety of roles in growth, development, inflammation and remodeling [28, 29]. MMPs also provide keratinocyte migration to perform re-epithelization on the damaged surface at wound edges in wound healing. In this study, the increment in MMP-9, collagen and cytokeratin expression levels mentioned above can be evaluated as an additional contribution to the strength of the connections between the intact and scar tissues, especially at the wound edges. Besides all these, observing the fact that PMF ensures tissue integrity earlier than the RF application can be considered as the superior of this method in terms of acute effect.

The Hif-1α/eNOS/VEGF signaling pathway, which is an important intracellular mechanism for the increase in vasodilation and growth factor synthesis underlying wound healing, is necessary to show the effectiveness of the therapeutic approaches that will be developed [30]. Activation of this pathway results in the synthesis of growth factors such as VEGF, which shows the formation of angiogenesis as well as vasodilation in the tissue. In this study, the wound healing capability of PMF and RF methods by applying separately and in combination was also examined by evaluating their outcomes on the Hif-1α/eNOS/VEGF pathway. Consistently with immunohistochemical results, the elevated mRNA expression levels of VEGF were detected in PMF and RF-applied groups on days 4 and 7. The hypothesis of this experiment was combined application of PMF and RF methods would be more effective for the wound healing process. Results of the genetical analyses showed that the co-application of PMF and RF increased the expression levels of eNOS, Hif-

1α and VEGF more effectively than their separate application. There is a fact that the activated Hif-1α/eNOS pathway with aforementioned cellular mechanisms in both methods also contributes to vascularization in addition to the other positive effects on scar tissue. Concerning the remarkable positive effects of PMF on this pathway is one of the aspects that increase the originality of the study.

Conclusion

In conclusion, our findings revealed that both in vitro PMF and RF applications can cause notable changes in factors that are required for tissue repair on wound healing such as epithelization, connective tissue formation, collagen production and angiogenesis. Considering all these data, further studies are needed to develop new types of devices including both methods that will support the repair of wound healing. Our evidentiary study of the production of such a device will shed light on many kinds of research related to wound healing.

Acknowledgments This study was supported by KOSGEB (project code 55FG1, Ispatya, Turkey) and Suleyman Demirel University Scientific Research Projects Coordination Unit (project code TSG-2022-8783) for consumable, analysis and animal costs required during experimental applications

Declarations

Conflict of interest The authors declare that they have no conflict of interests.

Ethical Approval The study was approved by the Suleyman Demirel University Experimental Animals Local Ethics Committee (Ethics No: 27.12.2019/14-02). All applicable institutional and/or national guidelines for the care and use of animals were followed.

References

1. Wilkinson HN, Hardman MJ (2020) Wound healing: cellular mechanisms and pathological outcomes. Open Biol 10:200–223
2. Yasukawa K, Okuno T, Yokomizo T (2020) Eicosanoids in skin wound healing. Int J Mol Sci 21:8435
3. Sivrice ME, Yasan H, Karahan N, Coban İ, Yetis A (2017) Effects of allantoin on wound healing in nasal mucosa. KBB-Forum 16(1):1–6
4. Sarataş B, Tüz M, Sivrice ME, Yasan H, Bozkurt KK (2019) Effects of platelet-rich plasma on wound healing in nasal mucosa. Med J Suleyman Demirel Univ 26(4):408–411
5. Schultz GS, Chin GA, Moldawer L, Diegelmann RF (2011) Principles of wound healing. In: Fitridge R, Thompson M (eds) Mechanisms of vascular disease: a reference book for vascular specialists. University of Adelaide Press, Adelaide (AU), p 23
6. Velnar T, Bailey T, Smrkolj V (2009) The wound healing process: an overview of the cellular and molecular mechanisms. J Int Med Res 37:1528–1542
7. Qing C (2017) The molecular biology in wound healing & non-healing wound. Chin J Traumatol 20:189–193
8. Ridiandries A, Tan JTM, Bursill CA (2018) The role of chemokines in wound healing. Int J Mol Sci 19:3217
9. Hu Y, Rao SS, Wang ZX, Cao J, Tan YJ, Luo J (2018) Exosomes from human umbilical cord blood accelerate cutaneous wound healing throughmiR-21-3p-mediated promotion of angiogenesis and fibroblast function. Theranostics 8:169–184
10. Hajialyani M, Tewari D, Sobarzo-Sánchez E, Nabavi SM, Farzaei MH, Abdollahi M (2018) Natural product-based nanomedicines for wound healing purposes: therapeutic targets and drug delivery systems. Int J Nanomed 13:5023–5043
11. Gaynor JS, Hagberg S, Gurfein BT (2018) Veterinary applications of pulsed electromagnetic field therapy. Res Vet Sci 119:1–8
12. Bragin DE, Statom GL, Hagberg S, Edwin MN (2014) Increases in microvascular perfusion and tissue oxygenation via pulsed electromagnetic fields in the healthy rat brain. J Neurosurg 122:1239
13. Guo JY, Yang T, Sun XG, Zhou NY, Li FS, Long D (2011) Ischemic postconditioning attenuates liver warm ischemia-reperfusion injury through Akt-eNOS-NO-HIF pathway. J Biomed Sci 18:79
14. Zhao J, Li YG, Deng KQ, Yun P, Gong T (2017) Therapeutic effects of static magnetic field on wound healing in diabetic rats. J Diabetes Res 630:5370
15. Eming SA, Martin P, Tomic-Canic M (2014) Wound repair and regeneration: mechanisms, signaling, and translation. Sci Transl Med. 6(265):265sr6
16. Bukowiecki A, Hos D, Cursiefen C, Eming SA (2017) Wound-healing studies in cornea and skin: parallels, differences and opportunities. Int J Mol Sci 18(6):1257
17. Lv H, Liu J, Zhen C, Wang Y, Wei Y, Ren W, Shang P (2021) Magnetic fields as a potential therapy for diabetic wounds based on animal experiments and clinical trials. Cell Prolif 54(3):e12982
18. Barchitta M, Maugeri A, Favara G, Magnano San Lio R, Evola G, Agodi A (2019) Nutrition and wound healing: an overview focusing on the beneficial effects of curcumin. Int J Mol Sci 20(5):1119
19. Gonzalez AC, Costa TF, Andrade ZA, Medrado AR (2016) Wound healing - A literature review. An Bras Dermatol 91(5):614–620
20. Albaugh VL, Mukherjee K, Barbul A (2017) Proline precursors and collagen synthesis: biochemical challenges of nutrient supplementation and wound healing. J Nutr 147:2011–2017
21. Ozgok Kangal MK, Regan JP (2020) Wound healing. StatPearls Publishing, Treasure Island
22. Kallis PJ, Friedman AJ (2018) Collagen powder in wound healing. J Drugs Dermatol 17(4):403–408
23. Song H, Gao K, Hao D, Li A, Liu R, Anggito B, Yin B, Jin Q, Dartora V, Lam KS, Smith LR, Panitch A, Zhou J, Farmer DL, Wang A (2023) Engineered multi-functional, pro-angiogenic collagen-based scaffolds loaded with endothelial cells promote large deep burn wound healing. Front Pharmacol 14:1125209. https://doi.org/10.3389/fphar.2023.1125209
24. Chattopadhyay S, Raines RT (2014) Review collagen-based biomaterials for wound healing. Biopolymers 101:821–833
25. Hu Z, Yang P, Zhou C, Li S, Hong P (2017) Marine collagen peptides from the skin of nile tilapia (Oreochromis niloticus): characterization and wound healing evaluation. Mar Drugs 15:102
26. Cheng Y, Hu Z, Zhao Y, Zou Z, Lu S, Zhang B (2019) Sponges of carboxymethyl chitosan grafted with collagen peptides for wound healing. Int J Mol Sci 20:3890

27. Vuong TT, Rønning SB, Ahmed TAE, Brathagen K, Høst V, Hincke MT (2018) Processed eggshell membrane powder regulates cellular functions and increase MMP-activity important in early wound healing processes. PLoS ONE 13:e0201975
28. Bove PF, Wesley UV, Greul AK, Hristova M, Dostmann WR, Vliet A (2007) Nitric oxide promotes airway epithelial wound repair through enhanced activation of MMP-9. Am J Respir Cell Mol Biol 36:138–146
29. Hingorani DV, Lippert CN, Crisp JL, Savariar EN, Hasselmann JPC, Kuo C (2018) Impact of MMP-2 and MMP-9 enzyme activity on wound healing, tumor growth and RACPP cleavage. PLoS ONE 13:e0198464
30. Zeng Z, Huang WD, Gao Q, Su ML, Yang YF, Liu ZC (2015) Arnebin-1 promotes angiogenesis by inducing eNOS, VEGF and HIF-1α expression through the PI3K-dependent pathway. Int J Mol Med 36:685–697

Publisher's Note Springer Nature remains neutral with regard to jurisdictional claims in published maps and institutional affiliations.

Springer Nature or its licensor (e.g. a society or other partner) holds exclusive rights to this article under a publishing agreement with the author(s) or other rightsholder(s); author self-archiving of the accepted manuscript version of this article is solely governed by the terms of such publishing agreement and applicable law.